C. HMS Cerenkov Blocking Corrections

The HMS threshold gas Cerenkov detector is used to ensure good e^-/π^- separation. In both F_π-1 and F_π-2, the HMS gas Cerenkov detector was used as a veto in the trigger for π^- runs in order to avoid high DAQ deadtime due to large e^- rates in the HMS. The effective gas Cerenkov thresholds used in the hardware veto are similar for both experiments, near two photoelectrons (see Fig. 7 for an example.) Since the actual veto threshold varies slightly from run to run due to PMT gain variations at high rates, slightly more restrictive software thresholds of $hcer_{npe} < 1.5$ and $hcer_{npe} < 2.0$ were applied in the analyses of the F_π-1 and F_π-2 data, respectively. Additionally in the F_π-2 experiment, an Aerogel Cerenkov detector was used for separating protons and π^+ for central momenta above 3 GeV/c.

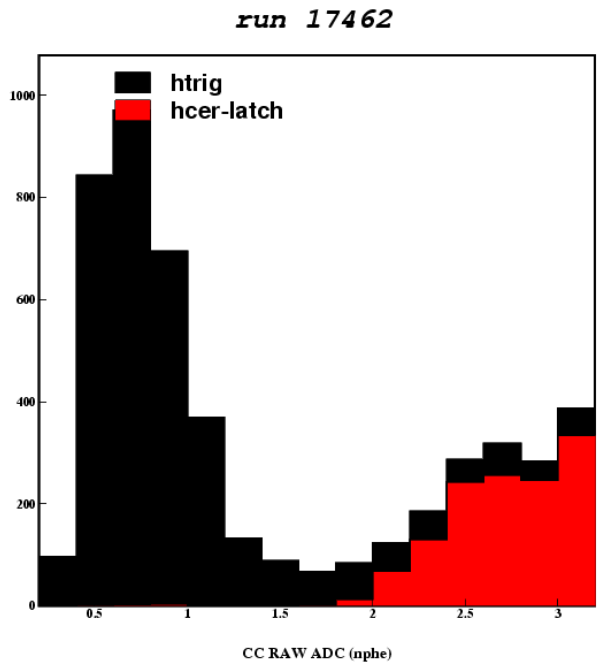

FIG. 7 A summed photoelectron histogram from the HMS Cerenkov for a representative F_π-1 carbon elastics run, ${}^{nat}C(e,e')$. The Čerenkov veto is not in the trigger; those events which would have been vetoed are indicated in red. The effective veto threshold appears to be at about 2.3 photoelectrons.

The loss of pions due to Cerenkov blocking is due to electrons passing through the gas Cerenkov within ≈ 90 ns after a pion has traversed the detector, resulting in a mis-identification of the pion event as an electron and being eliminated by the analysis cuts applied. Thus, the correct estimation of the gas Cerenkov blocking correction is essential in extracting the π^- cross section and is implicit in the final estimation of π^-/π^+ ratios of separated response functions.

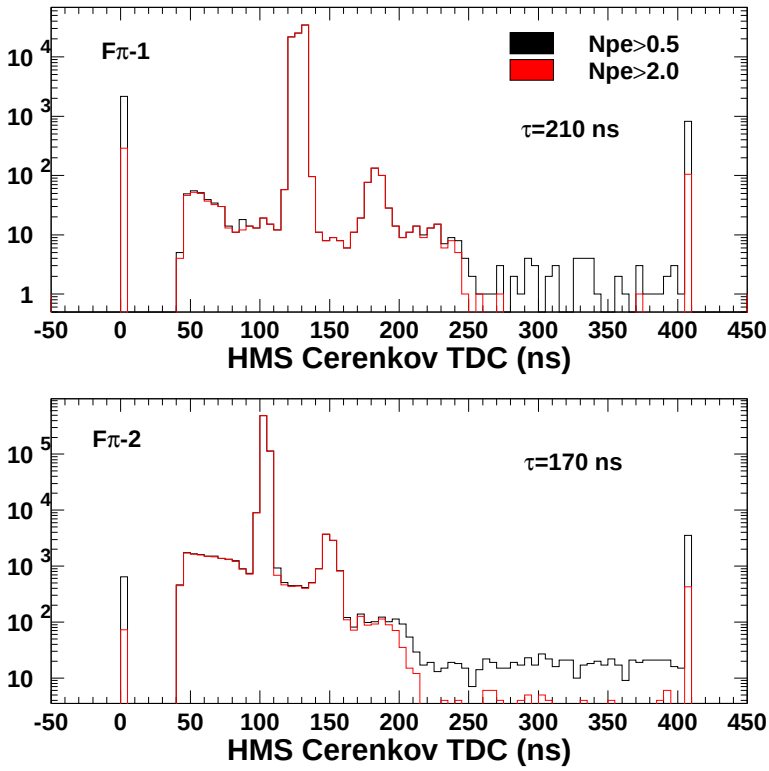

FIG. 8 Gas Cerenkov TDC open trigger spectrum for F_π-1 (upper panel) and for F_π-2 (lower panel). The data are taken from a deuterium π^- coincidence run where the HMS trigger was 3/4 (no PID). A cut is then placed on the number of Cerenkov photoelectrons to select "electron" events.

Fig. 8 shows HMS Cerenkov TDC spectra for photoelectron requirements of $N_{phe} > 0.5$ (black line) and $N_{phe} > 2.0$ (red line) [F_π-1 (upper panel), F_π-2 (lower panel)]. The TDC is started by the HMS pretrigger signal and is stopped by the retimed (i.e. delayed and disciminated) Cerenkov signal. The main peak corresponds corresponds to signals from electrons that result in the trigger, as identified by the Cerenkov ADC. Events not associated with the original trigger (other electrons, or pions that are mis-identified as electrons due to Cerenkov blocking) appear as additional events to the left and right of the main electron peak in the TDC spectra. The second peak to the right is due to a second electron arriving within the timing window, but after the discriminator "dead window" of 50-60 ns (caused by the length of the discriminator pulse). The backgrounds to the left and right of the two peaks are due to earlier and later electrons, while the tail extending to 410 ns is due to pedestal noise that crosses the 0.5 p.e. threshold. Zeros correspond to electrons (or pions) that may not have satisfied the 3/4 condition, or that come from the tail end of a Cerenkov pulse from a previous event.

While the events to the left of the main peak correspond to early electrons passing through the detector before the electrons associated with the trigger (already addressed in the coincidence time blocking correction), the events to the right of the main peak correspond to electrons traversing the detector after the original trigger electrons. The later events are used to estimate the Cerenkov blocking efficiency, $\delta_{CCblock}$, from the electron rate into the HMS and the effective Cerenkov TDC gate width ($\approx$ 100 ns),

$$\delta_{CCblock} = e^{-R_e * \tau_{eff}}. \tag{8}$$

Here, R_e denotes the HMS electron rate as measured by the ELCLEAN scaler, while the effective Cerenkov gate width τ_{eff} ns is determined from the dependence of $\delta_{CCblock}$ upon R_e.

During the F_π-2 negative polarity data taking, dedicated runs were taken for all π^- kinematic settings except Q^2=2.45, high ϵ, E_e = 5.25 GeV, θ_{HMS} = 13.61. A variety of electron beam currents were used in order to determine the Cerenkov blocking correction versus electron rate into the HMS. Cuts of

$$abs(hsdelta) < 8.0 \qquad abs(hsxptar) < 0.09 \qquad abs(hsyptar) < 0.055 \qquad hcer_{npe} < 2.0 \tag{9}$$

were applied to ntuples from each of these runs, resulting in the data tabulated in Table I.

The normalized pion yield $SING * PS1 + COIN$ was calculated for each run, where the SOS electronic live time was applied only to $COIN$. To determine whether the extracted blocking factors are consistent for the different sets of kinematics, each set was fit to a function of the form $Y = A^{-R\tau}$. Although A introduces an additional free parameter to the fit, this allows τ to be extracted for each set without being sensitive to the normalization of the 'low rate yield'. As shown in Figs. 9, 10, the obtained gate widths are reasonably independent of kinematic setting. Because the runs at Q^2=2.45, high ϵ, $E_e = 5.25$ GeV, $\theta_{HMS} = 16.61$ are only at low rates, that τ value is not shown. The fit τ_{eff} values are significantly larger than the measured Cerenkov TDC gate width (= 85 ns for F_π-1 and = 100 ns for F_π-2). This effect may be explained in terms of the intrinsic width of the Cerenkov signal. While the ADC gate is fixed, the Cerenkov signal itself has some width and the overlap determines an effective gate width.

Since the τ values for the different kinematic settings are reasonably consistent, a combined fit of all of the data was made. In this case, the data for each kinematic setting were separately renormalized until A for each was close to unity. This effectively removes the cross section variation with kinematics. The combined fits to the renormalized data are shown by the black lines in Figs. 9, 10. These combined fits unavoidably depend on the renormalization constants chosen for the four

Run	Q_{tot} (μC)	Rate (kHz)	PS1	htr	cpult	hele	sele	SING	COIN
Q^2=2.45, low ϵ, $E_e = 4.21$ GeV, $\theta_{HMS} = 10.54$									
47190	35632	536	1978	0.966	0.905	0.959	0.9993	2999	5654
47191	21863	312	596	0.973	0.917	0.977	0.9996	6926	2171
47192	10301	153	299	0.979	0.935	0.989	0.9998	6990	608
47241	27317	522	989	0.966	0.879	0.959	0.9993	4478	4048
47242	17066	500	989	0.966	0.880	0.960	0.9993	2768	2529
47243	15933	306	298	0.973	0.867	0.977	0.9996	9435	1495
47244	12196	307	298	0.973	0.867	0.977	0.9996	7294	1125
47245	6118	150	99.7	0.979	0.844	0.989	0.9998	11098	283
47246	5437	152	99.7	0.979	0.840	0.989	0.9998	9722	267
Q^2=2.45, low ϵ, $E_e = 4.21$ GeV, $\theta_{HMS} = 12.21$									
47266	56228	358	993	0.972	0.901	0.973	0.9990	4876	6181
47267	32848	217	398	0.977	0.916	0.984	0.9994	7597	2390
47296	10513	69.3	99.9	0.982	0.923	0.995	0.9998	10298	284
47297	49966	390	991	0.970	0.874	0.969	0.9988	4195	6454
Q^2=2.45, high ϵ, $E_e = 5.25$ GeV, $\theta_{HMS} = 10.61$									
47479	8088	63.8	20.0	0.970	0.808	0.999	0.9997	224609	2437
47480	9204	64.4	145	0.980	0.885	0.995	0.9997	37467	3070
47481	3327	63.8	99.8	0.980	0.843	0.995	0.9997	19187	1099
47483	38898	315	992	0.970	0.767	0.972	0.9984	18793	43638
Q^2=2.45, high ϵ, $E_e = 5.25$ GeV, $\theta_{HMS} = 16.61$									
47509	6616	6.75	10.0	0.982	0.849	0.999	0.9997	36621	367
47510	65033	50.6	59.9	0.978	0.782	0.996	0.9977	54716	12984
47511	14012	51.1	59.9	0.975	0.782	0.996	0.9976	11820	2782

TABLE I HMS Cerenkov blocking study data taken during F_π-2 π^- data taking. The rate is calculated from the ELCLEAN scaler, divided by the average of beam on times 1 & 2 (Threshold cuts: 5 μA for BCM 1 and 1 μA for BCM 2). The last two columns are the number of HMS singles and coincidences passing the cuts listed in Eqn. 9. Note that run 47482 was not included in this study, since its cpult was anomalously low for easily justifiable reason, and so seemed suspect.

kinematic settings, but the methodology employed does not allow too much arbitrary judgement. With only one exception, the τ value for the combined data fit is consistent with the fits to each kinematic setting separately.

The τ_{eff} value and its uncertainty used in the CC blocking correction was estimated from the four fits shown in Fig. 9. Taking into account the respective uncertainty in these four fits yields a central value of $\tau_{eff} = 249.8 \pm 12.6$ ns. This value is used to compute the CC blocking corrections used for the F_π-2 data normalization, shown as a function of the electron rate in Fig. 11. Also shown are the blocking corrections that would have been obtained if τ_{eff} was raised or lowered by its uncertainty. The mean deviation in CC blocking correction, determined over the range of actual rates encountered in the F_π-2 experiment is XXX%.

For the F_π-1 data, a slightly different procedure was used. Open trigger data at different electron rates were unfortunately not taken during this experiment, so the Cerenkov blocking correction could not be directly determined for those data. We used the TDC timing information from the

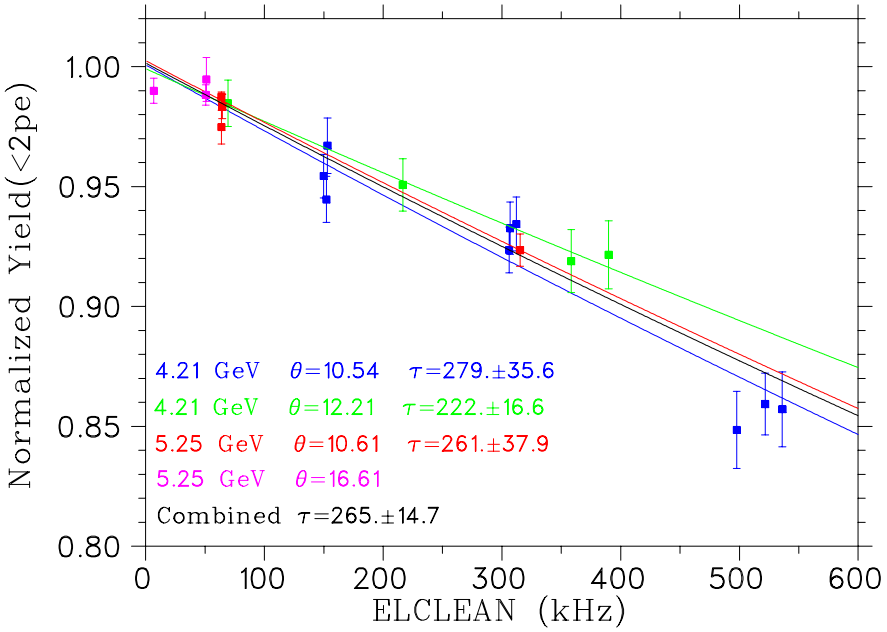

FIG. 9 Normalized experimental yields taken during an open trigger (3/4 SCIN) singles run, with a $N_{p.e.} > 2.0$ Cerenkov particle identification cut applied, as a function of electron rate in the HMS. The colored lines are fits of the form $Y = A^{-R\tau}$ for each kinematic setting separately. The black line is a combined to all of the data, as explained in the text. The fit value for τ_{CC} is larger than the measured Cerenkov TDC gate width (≈100 ns, dashed line). This discrepancy is attributed to the width of the Cerenkov signal, whose overlap with the ADC gate determines an effective gate width.

only F_π-1 "open trigger" run taken just before the main data taking to estimate the scaling with respect to the F_π-2 timing information. As shown in Fig. 8, the TDC timing window used during F_π-1 was 210 ns, while for F_π-2 it was 170 ns, a difference of 23%. The ratio of these values was used as the scaling factor for the TDC Cerenkov effective gate width for F_π-1 with respect to the F_π-2 TDC gate width. To estimate the F_π-1 blocking correction, a $N_{p.e.} < 1.5$ cut was applied to the F_π-2 data, yielding the τ values shown in Fig. 10, and a central value of 282.9 ± 11.0 ns. We then scaled this according to the F_π-1 TDC time window, yielding a value of $\tau_{eff} = 348.4 \pm 8.5$ ns. This value is used to compute the CC blocking corrections used for the F_π-1 data normalization, shown as a function of the electron rate in Fig. 12. The size of the Cerenkov blocking correction ranges from 2% to ∼YY% for the highest electron rate data. The mean deviation in CC blocking correction, determined over the range of actual rates encountered in the F_π-1 experiment is XXX%. The Cerenkov effective TDC gate width varied by 4-5 ns, a 1% effect. We added to this error in quadrature the systematic uncertainty due to the F_π-1/F_π-2 TDC time window (trigger hardware initial setup) scaling (±0.5 ns), the uncertainty due to the HMS tracking efficiency (1-2 ns), and the uncertainty to the combined fit resulting in an overall uncertainty of XXX%.

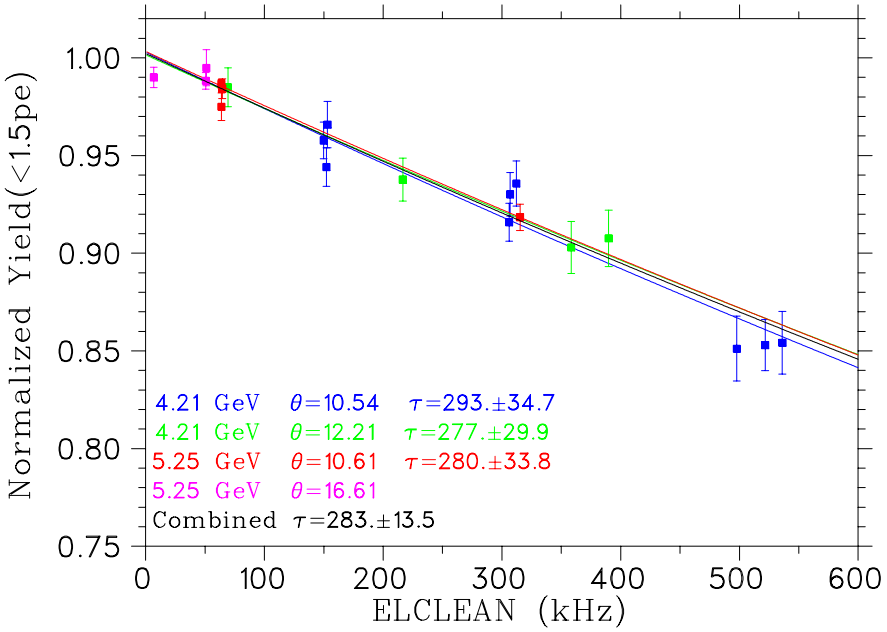

FIG. 10 Same as Fig. 9, except that a $N_{p.e.} > 1.5$ Cerenkov particle identification cut is applied.

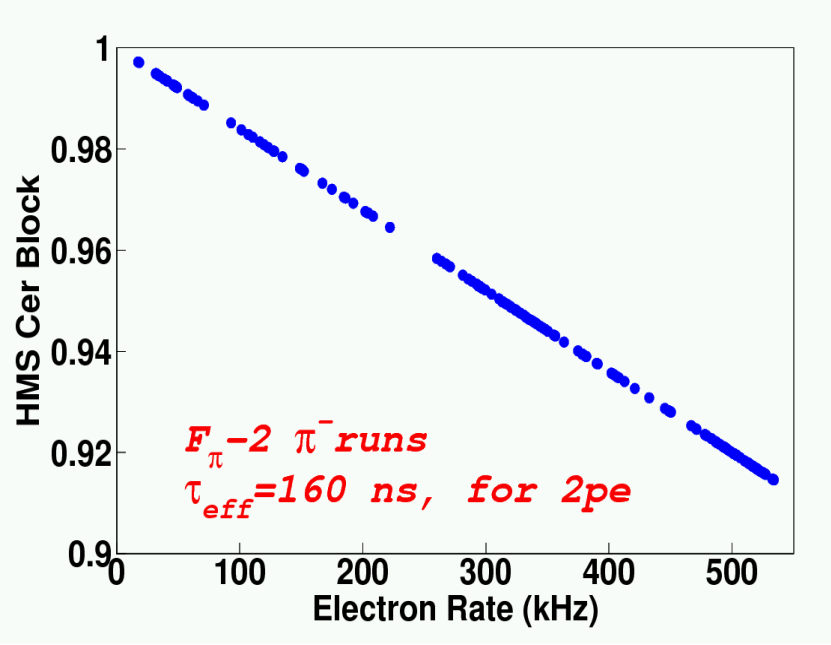

FIG. 11 F_π-2: HMS Cerenkov blocking correction $\delta_{CCblock}$ plotted as a function of the electron rate R_e. At high rates (≈600 Hz) the correction is at the level of 9%. **THIS FIGURE IS NOT YET UPDATED FOR THE NEW BLOCKING CORRECTION. THIS WILL ONLY BE DONE ONCE WE HAVE AGREED THAT THE METHODOLOGY FOR DETERMINING THE CORRECTION IS REASONABLE.**

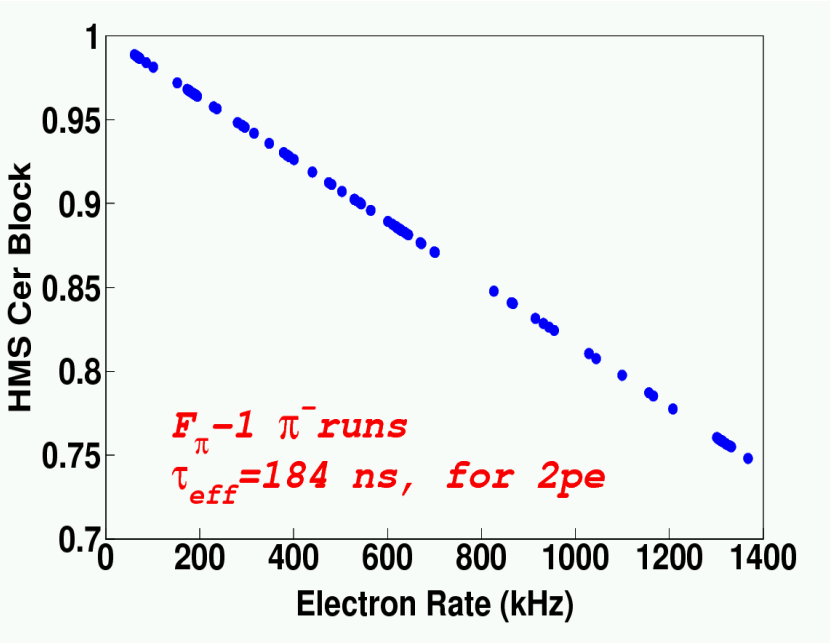

FIG. 12 F_π-1: HMS Cerenkov blocking correction $\delta_{CCblock}$ plotted as a function of the electron rate R_e. At high rates ($\approx$1.4 MHz), the correction is at the level of 25%. **THIS FIGURE IS NOT YET UPDATED FOR THE NEW BLOCKING CORRECTION!**